Electronic Supplementary Material (ESI) for Journal of Materials Chemistry B.

Supporting Information

A Schiff's base receptor for the Red fluorescence live cell imaging of Zn^{2+} ions in Zebrafish embryos and Naked eye detection of Ni^{2+} ions for bio-analytical Applications

A. Senthil Murugan[a], N. Vidhyalakshmi[b], U. Ramesh[b] and J. Annaraj[a]*

[a]Depertment of Materials Science, School of Chemistry, Madurai Kamaraj University, Madurai-21

[b]Department of Molecular biology, School of biological Sciences, Madurai Kamaraj University, Madurai-21

S.No	Contents	Page.No
1	General information about UV-vis and fluorescent spectroscopy experiments	3
2	Determination of the Binding constant	3
3	Determination of the Limit of Detection	3
4	Synthesis of 3-formyl-2-hydroxy quinoline	4
5	Experimantal Producere for MTT assay	4
6	^{1}H NMR spectrum of the QAMP (Figure S1)	5
7	^{13}C NMR spectrum of the QAMP (Figure S2)	5
8	ESI-MS spectrum of QAMP (Figure S3)	6
9	Photograph of Fluorometric and colorimetric response of the QAMP with Metal ions (Figure S4)	6
10	Linear fit for QAMP with Zn^{2+} in fluorescence spectroscopy (Figure S5)	7
11	Determination of the binding constant value of Zn^{2+} with QAMP by B-H plot analysis from fluorescence titration (Figure S6)	7
12	ESI-Mass spectroscopy of QAMP-Zn (Figure S7)	8
13	Linear fit for QAMP with Ni^{2+} in UV-vis spectroscopy (Figure S8)	8
14	Determination of the binding constant value of Ni^{2+} with QAMP by B-H plot analysis from UV-vis titration (Figure S9)	9
15	ESI-Mass spectroscopy of QAMP-Ni (Figure S10)	9
16	Fluorescence spectral data for molecular logic circuit (Figure S11)	10
17	Cytotoxicity of QAMP against AGS lungs cancer cell (Figure S12)	10
18	Selectivity spectrum of the QAMP with various anions in UV-vis spectroscopy (Figure S13)	11
19	Interference study of QAMP-Ni ion with various anions in UV-vis spectroscopy (Figure S14)	11
20	Selectivity spectrum of the QAMP with various anions in fluorescence spectroscopy (Figure S15)	12
21	Interference study of QAMP-Ni ion with various anions in fluorescence spectroscopy (Figure S16)	12
22	Mortality of QAMP to Zebrafish embryos (Figure S17)	13
23	Mortality of Zn^{2+} ions to Zebrafish embryos (Figure S18)	13
25	Comparison Table (Table S1)	14
26	References	15

1. Determination of the Binding constant.

The binding constant value of Ni^{2+} and Zn^{2+} with QAMP has been determine by using UV-vis and Fluorescence spectrometer respectively. The concentration of the QAMP was constant throughout experiments and varying the concentration of the Ni^{2+} and Zn^{2+} gives linear relationship. The constant value of Ni^{2+} with QAMP was determined by using Benesi-Hildebrand equation[1].
Ka was calculated following the equation stated below.

$$1/(A-A_o) = 1/\{K(Amax–A_o)\ [Ni^{2+}]\} + 1/[Amax-A_o]$$

Here,
A_o is the absorbance of receptor in the absence of guest,
A is the absorbance recorded in the presence of added Ni^{2+} ions,
Amax is absorbance in presence of added $[Ni^{2+}]$max and K is the association constant (M^{-1}). The association constant (K) could be determined from the slope of the straight line of the plot of $1/(A-A_o)$ against 1/[Ni]. The association constant (*Ka*) as determined by UV-vis titration method.

Determination of the Binding constant value of the Zn^{2+} with QAMP were determine by using modified Benesi-Hildebrand equation stated below,

$$1/\ I\text{-}Imin = 1/\ Imax\text{-}Imin + (1/K[C])(1/\ Imax\text{-}Imin).$$

Where,
Imin, I, and Imax are the emission intensities of QAMP, at an intermediate Zn^{2+} concentration with QAMP, and at a concentration of complete saturation, K is the binding constant and [C] is the Zn^{2+} concentration respectively. From the plot of (Imax-Imin)/(I-Imin) against $[C]^{-1}$ for **QAMP-Zn**, the value of K has been determined from the slope.

2. Determination of Limit of Detection (LOD)

LOD for Ni^{2+} and Zn^{2+} ions with QAMP were determined by UV-Vis and Fluoromentric titrations using the formulae **3σ/slope**, here, σ is standard division of the Black solutions (probe alone) and slope was derived from titration curve.

3. Synthesis of 2-hydroxy-3-formyl quinoline

$POCl_3$ and DMF (3:1) were placed in an ice bath. Add to this 1eq of phenylacedamide and allow to stirring in a room temperature for 30 mints. A brown colour solution was allowed to reflux under stirring for 6hr at 80^0c. The reaction solution was poured in to crushed ice and a yellow colour precipitated was filleted, dried and recrystallize with ethyl acetate. The aldehyde was used further reaction without any purification. 2-chloro substituted quinoline aldehyde was dissolved in acetic acid and water mixture (7:3) and reflux for 2 hr. During the refluxation the acetylation followed by hydrolysis was occurred. Poured to ice and filtered, a yellow coloured aldehyde was used for the Schiff base formation.

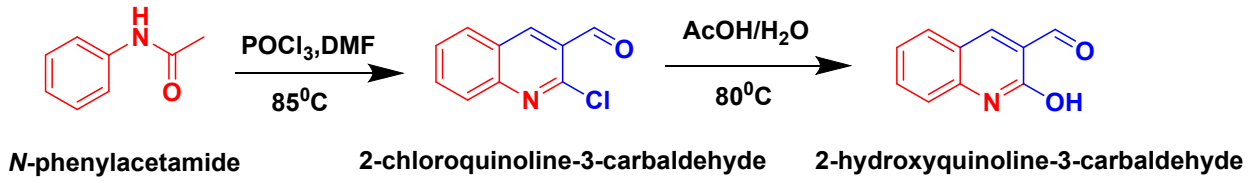

Scheme S1: Synthesis of 2-hydroxyquinoline-3-carbaldehyde

4. Experimantal Producere for MTT assay

The A549 cancer cells were seeded at the concentration of $1x10^4$ cells in 96 well plates and incubated for 48 hours in incubator with 5% of CO_2 at 37°C and the receptor QAMP (0-50 μM). After 48 hours of treatment with series of concentration of receptor, MTT was added to each well at 0.5 mg/ml concentration. After incubation for 4 hours in CO_2 incubator, media was carefully removed and the purple formazan precipitate was dissolved in 100 ml/well DMSO and kept incubator for 15 min in dark. Estimation of formazan product was performed at 570 to 690 nm in a micro-plate reader. This assay was performed in triplicates. The data was plotted against the receptor concentration and the relative cell viability (%) in comparison to the control cells.

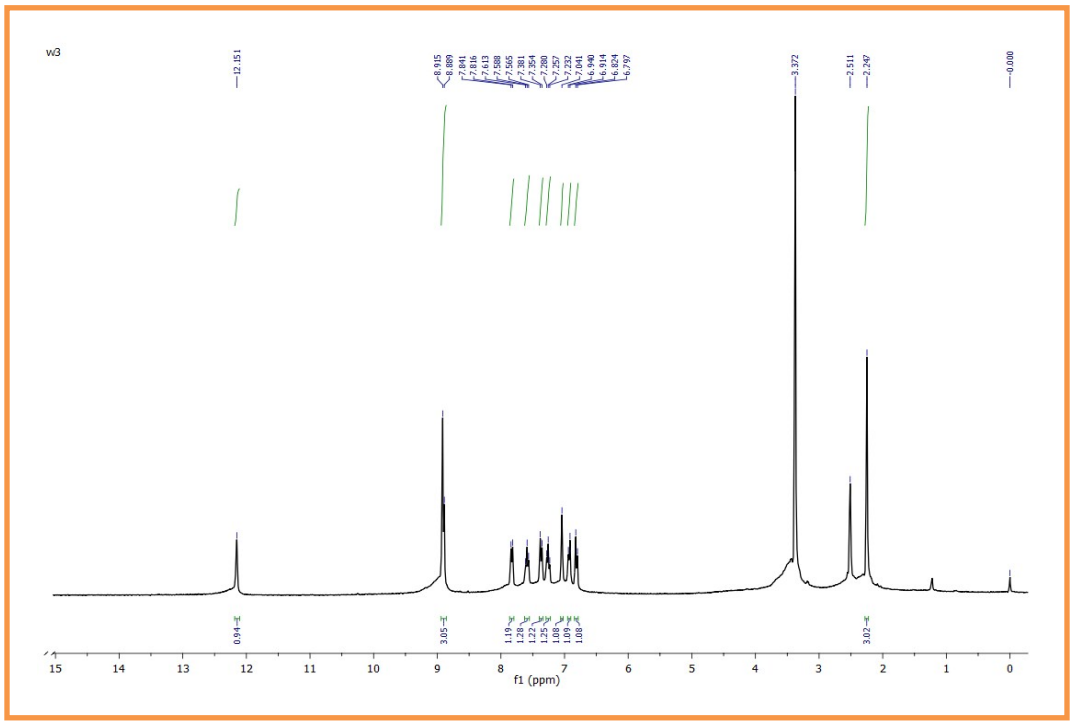

Figure S1: ^{1}H NMR spectrum of the QAMP in DMSO-d^{6}

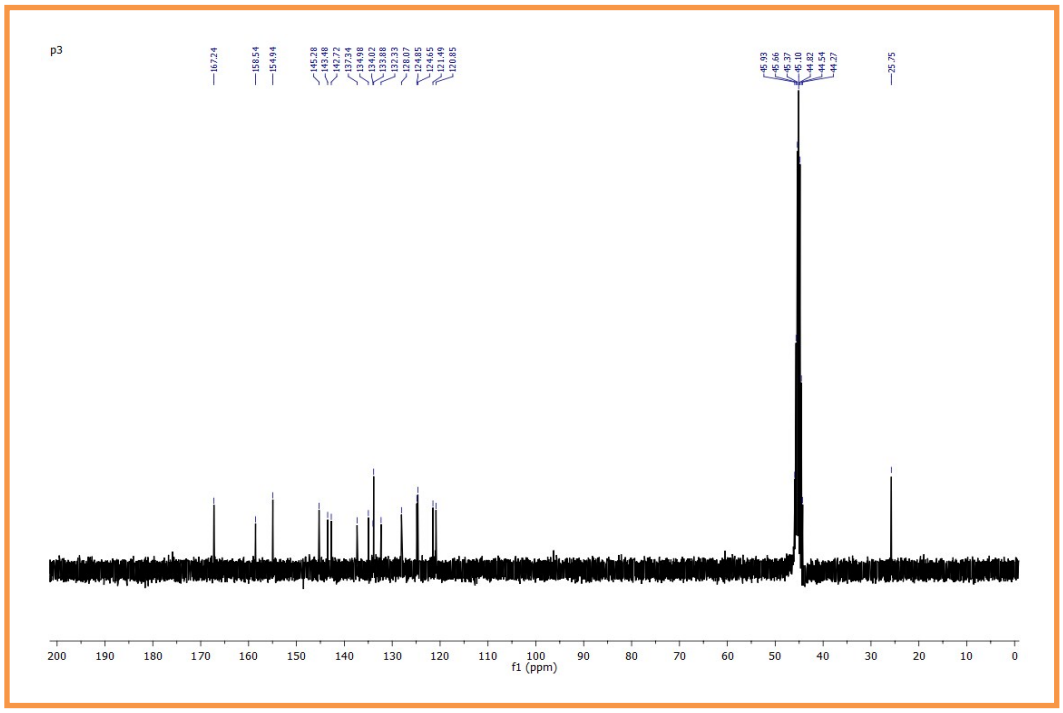

Figure S2: ^{13}C NMR spectrum of the QAMP in DMSO-d^{6}

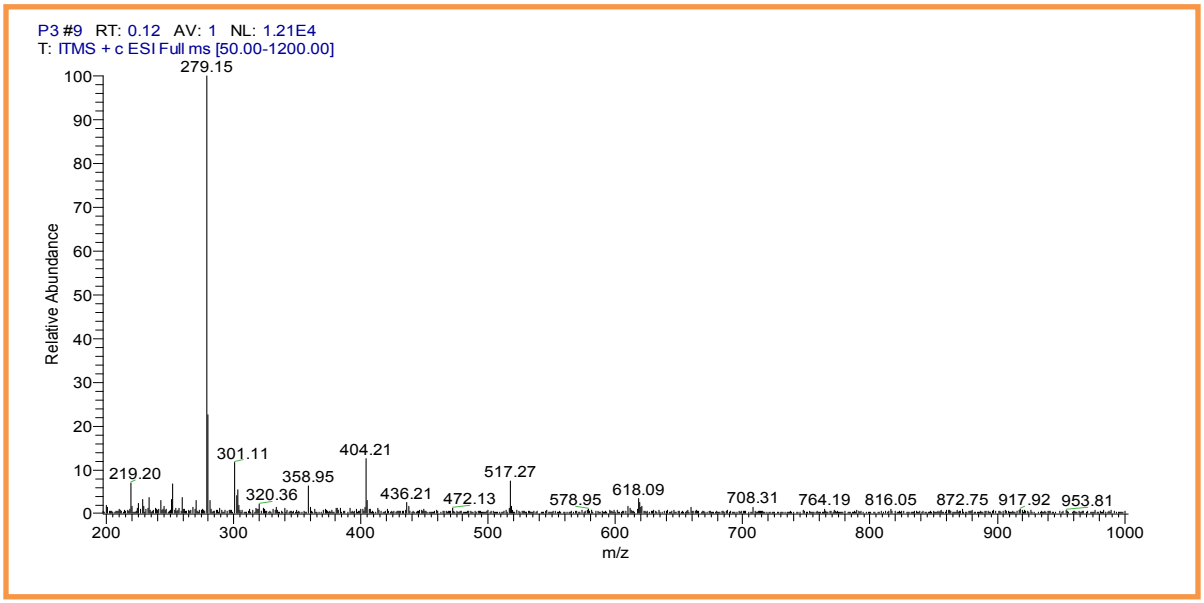

Figure S3: ESI-MS spectrum of QAMP in Methanol

Figure S4: Photograph of (a) Fluorometric and (b) colorimetric response of QAMP (50 μM) with 10 equiv of Metal ions. QAMP, Zn^{2+}, Ni^{2+}, Cu^{2+}, Mn^{2+}, Co^{2+}, Pb^{2+} and Hg^{2+}(Top left-right), Fe^{2+}, Fe^{3+}, Al^{3+}, In^{3+}, Mg^{2+}, Ca^{2+}, and Ba^{2+}. (Bottam left-right).

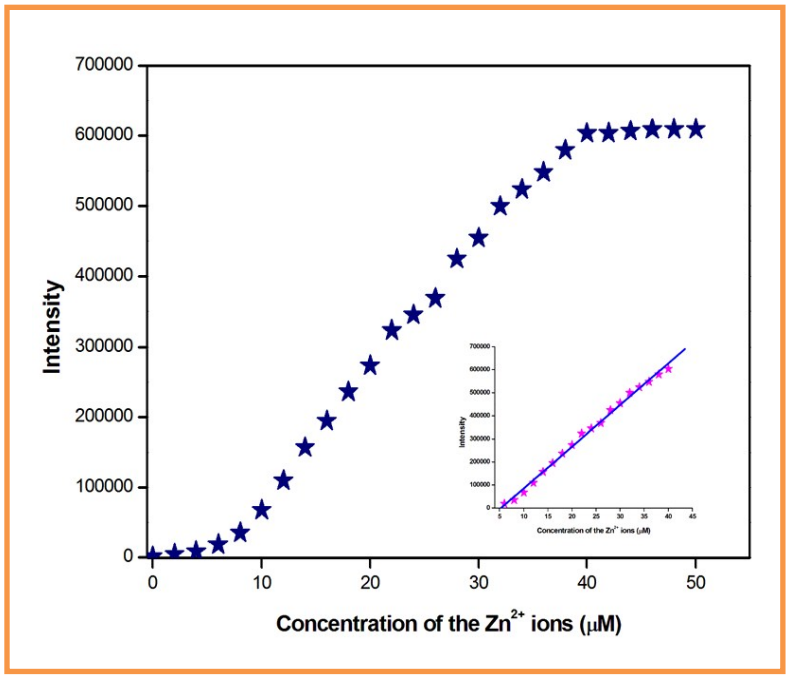

Figure S5: Linear fit for QAMP with Zn^{2+} in fluorescence spectroscopy (inside linear fit plot). Intensity measured at 663 nm.

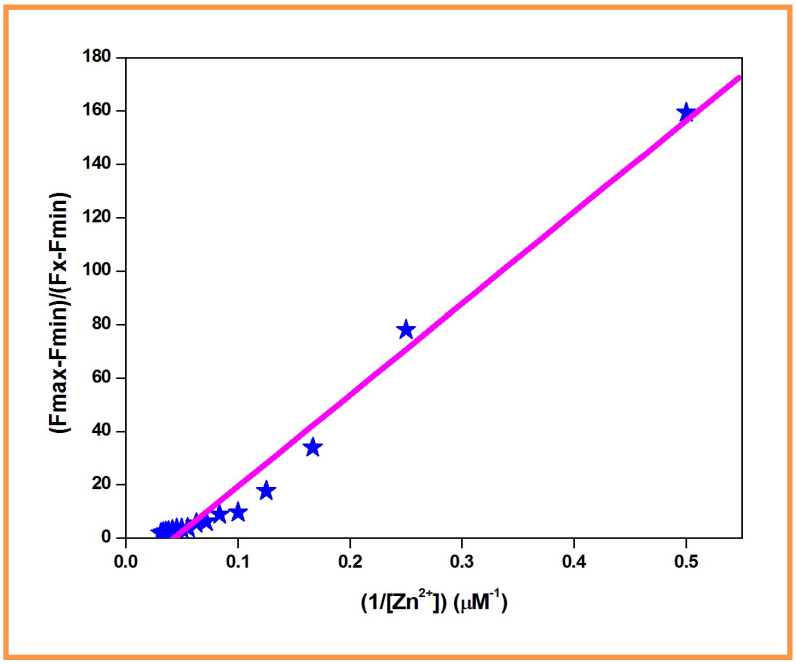

Figure S6: Determination of the binding constant value of Zn^{2+} with QAMP by B-H plot analysis from fluorescence titration. Intensity measured at 663 nm.

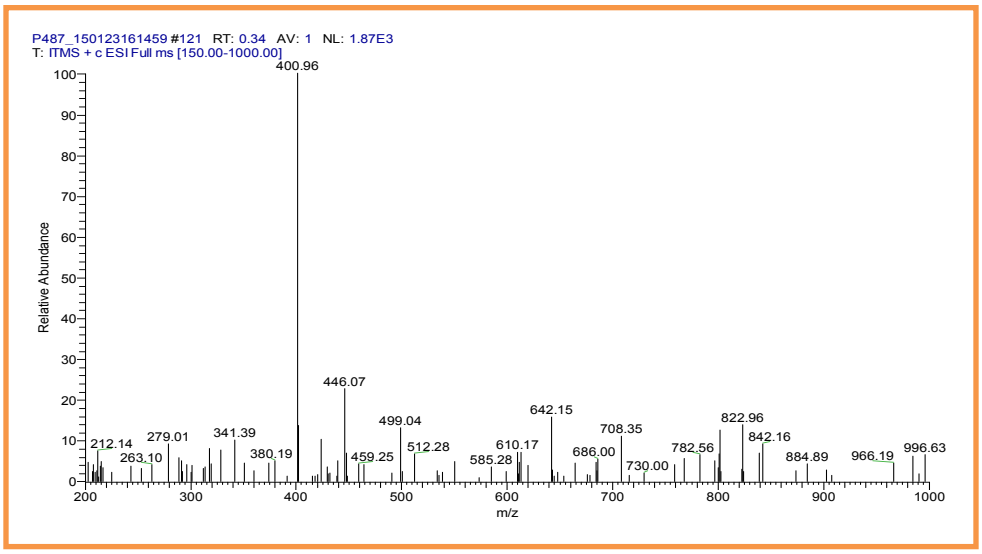

Figure S7: ESI-Mass spectroscopy of QAMP-Zn in methanol

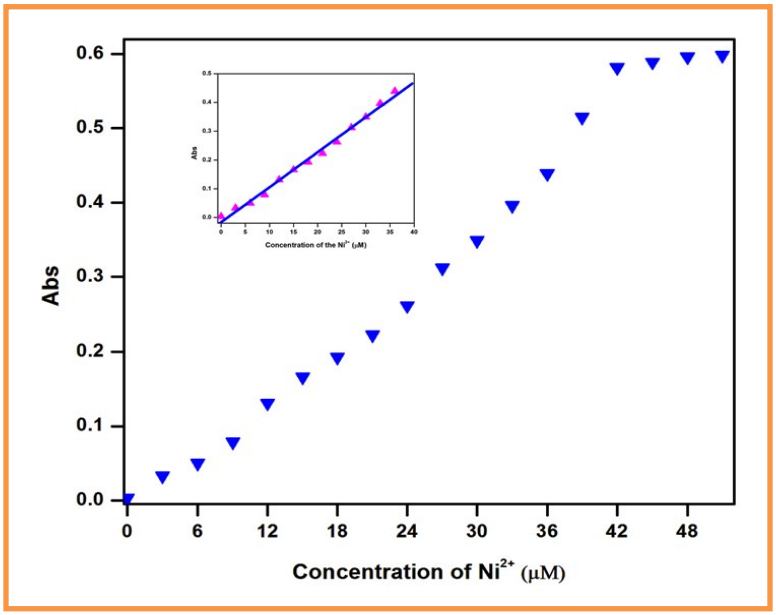

Figure S8: Linear fit for QAMP with Ni^{2+} in UV-vis spectroscopy (inside linear fit plot). Absorbance measured at 523 nm

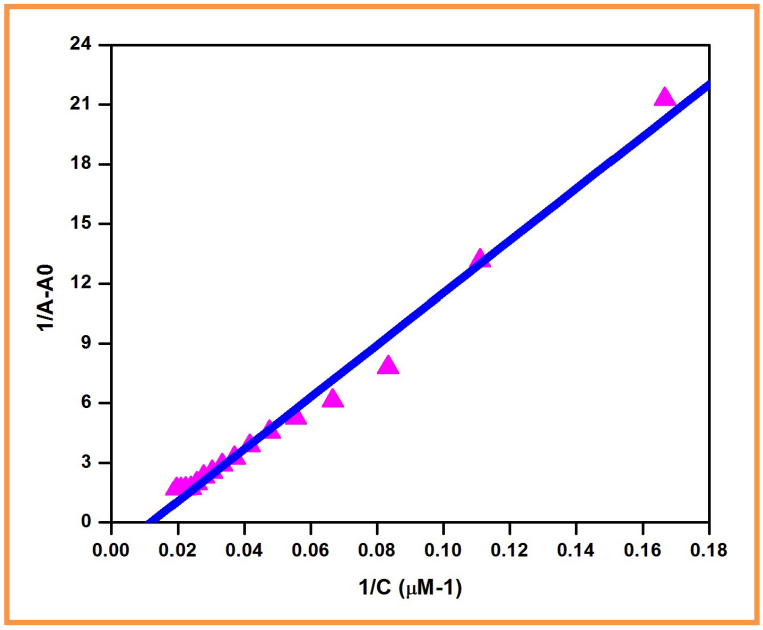

Figure S9: Determination of the binding constant value of Zn^{2+} with QAMP by B-H plot analysis from fluorescence titration. Absorbance measured at 523 nm.

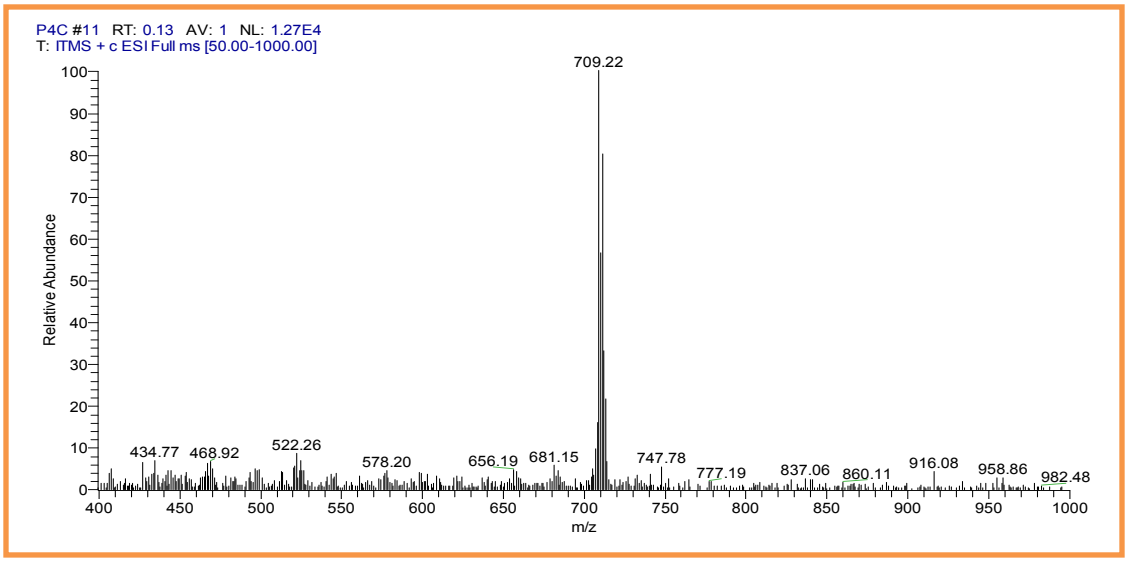

Figure S10: ESI-Mass spectroscopy of QAMP-Ni in methanol

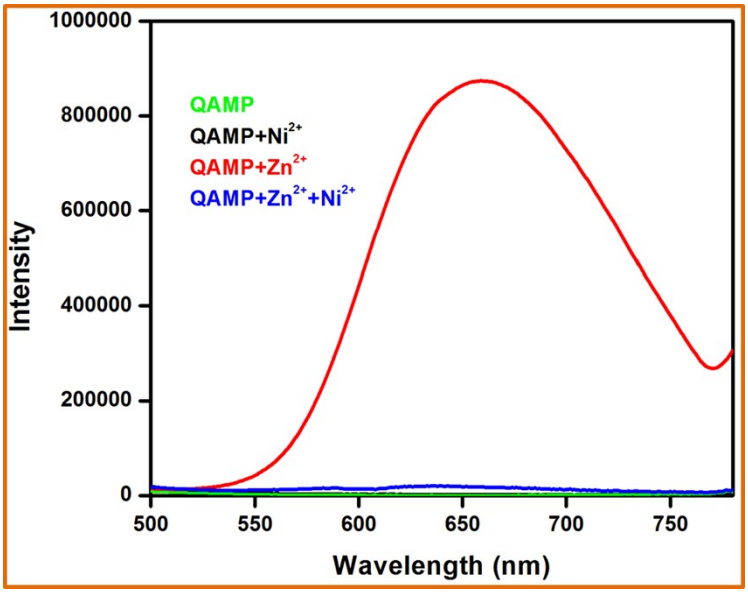

Figure S11: Fluorescence Spectral Data for Molecular logic circuit

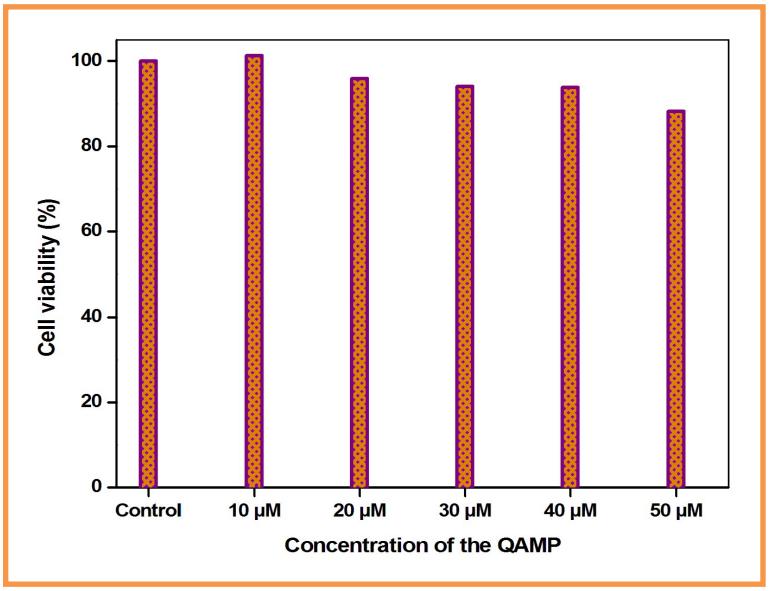

Figure S12: Cytotoxicity of QAMP against AGS lungs cancer cell

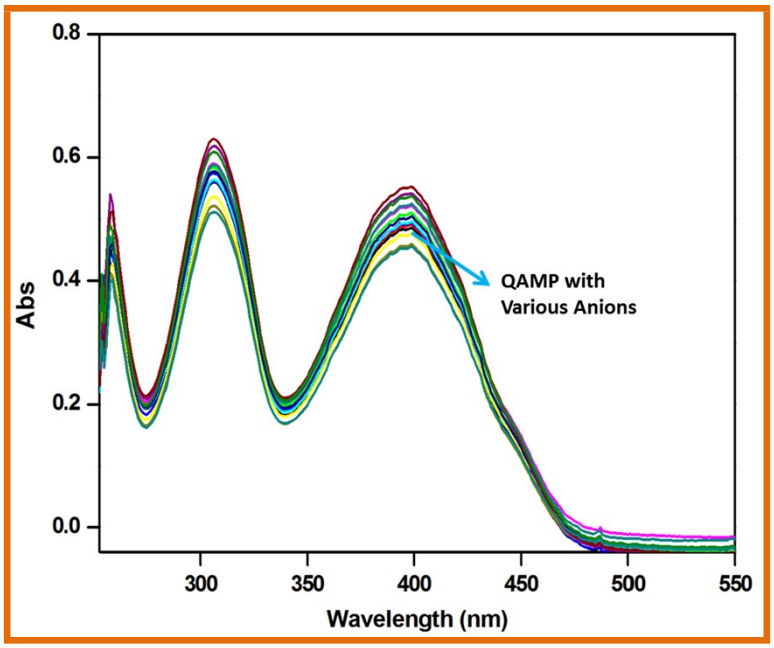

Figure S13: Selectivity spectrum of the QAMP with 10 equiv of various anions in UV-vis Spectrum.

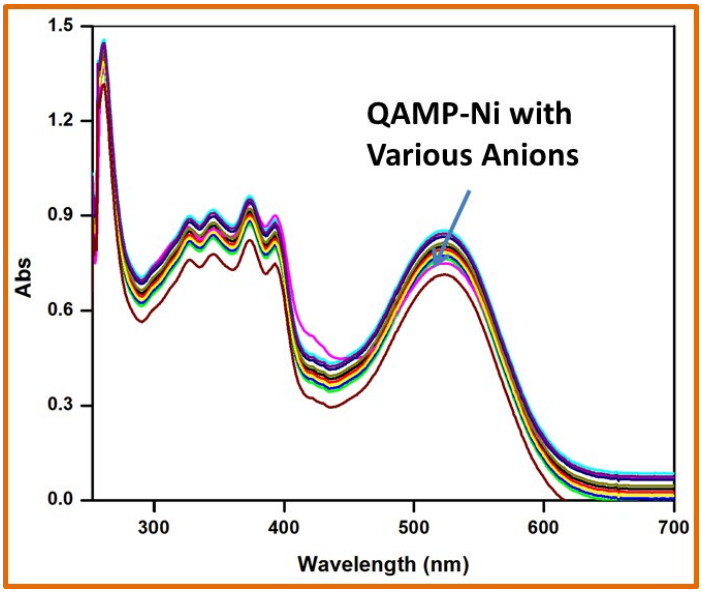

Figure S14: Interference study of QAMP-Ni ion with various anions in UV-vis spectrum

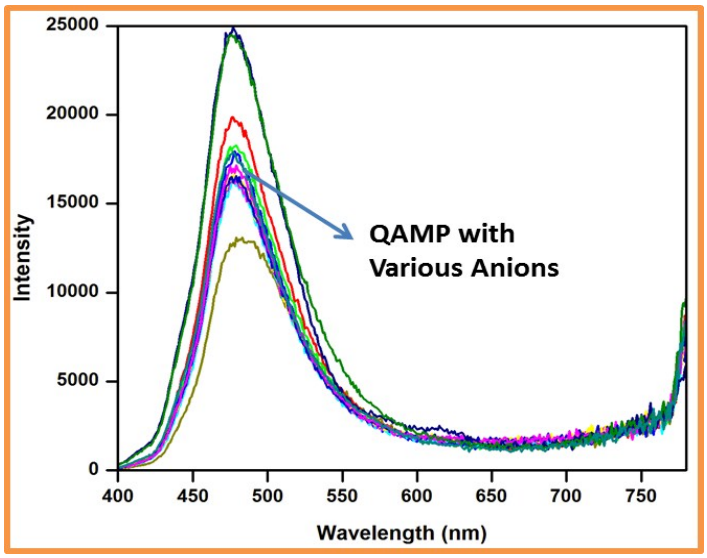

Figure S15: Selectivity spectrum of the QAMP with 10 equiv of various anions in fluorescence Spectrum.

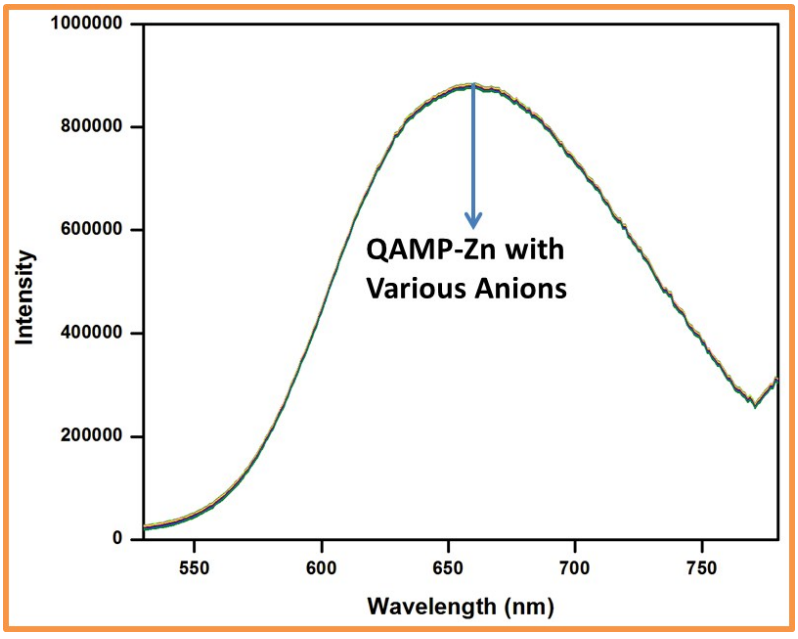

Figure S16: Interference study of QAMP-Zn ion with various anions in fluorescence spectroscopy

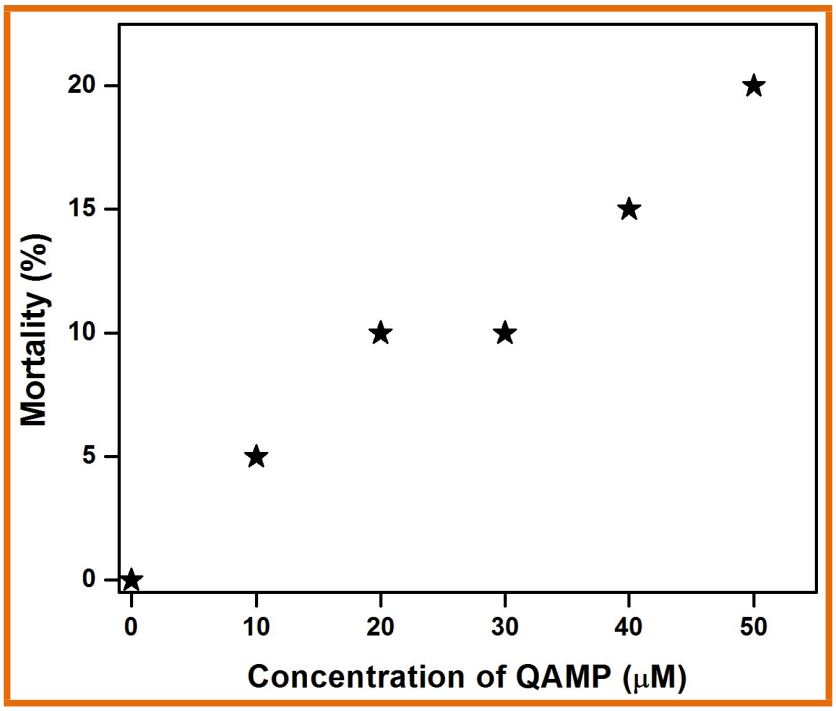

Figure: S17 Mortality of QAMP to Zebrafish embryos

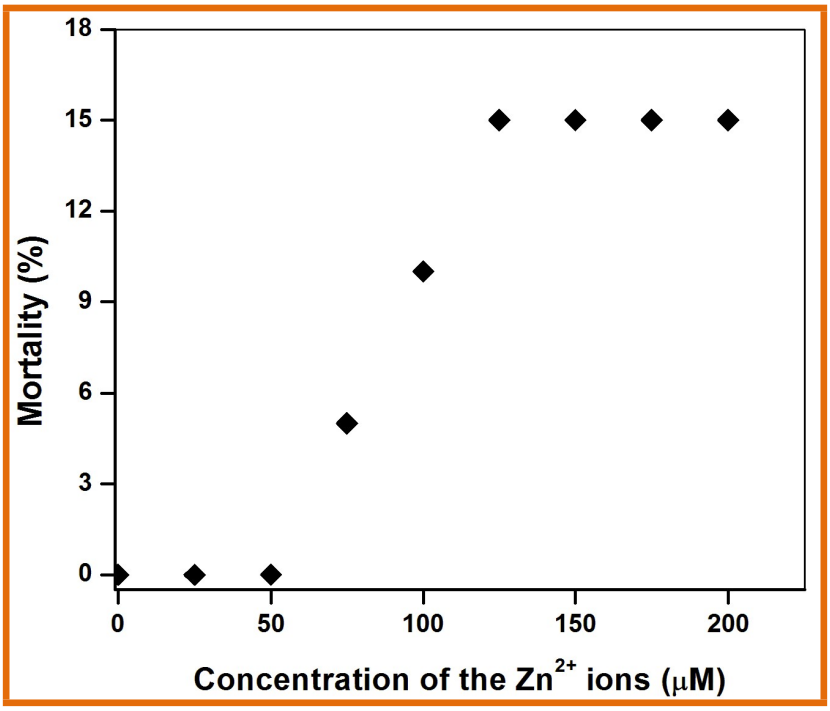

Figure: S18 Mortality of Zn^{2+} ions to Zebrafish embryos

Table S1 Comparison Table

S.No	Probe	Analytes	LOD (μM)	Application	Ref
1	Calix[4]arene based chemosensor	Zn(II) and Ni(II)		---	2
2	Benzo[*d*]thiazole based chemosensor	Zn(II)	0.112	Real Sample Analysis	3
3	8-Amino Quinoline based chemosensor	Zn(II) and Co(II)	Zn(II)-0.01 Co(II)- 6.89	Fluorescence imaging of fibroblasts	4
4	Pyrimidine based chemosensor	Zn(II)	0.97	Fluorescence cell imaging on HeLa cells	5
5	Julolidine based chemosensor	Zn(II) and Co(II)	Zn(II)-0.8 Co(II)-0.34	--	6
6	Schiff Base	Ni(II)	0.5	---	7
7	Pyridoxal based chemosensor	Cu(II) and Zn(II)	Cu(II)-0.14 Zn(II)-0.021	Fluorescence cell imaging on HepG2 cells	8
8	Naphthalenediols based chemosensor	Cu(II) and Ni(II)	0.01 for both	---	9
9	Naphthaldehyde based chemosensor	Zn(II)	0.11	On site analysis	10
10	Quinoline based chemosensor	Zn(II) and Ni(II)	Zn(II)-0.078 Ni(II)-0.37	Live cell imaging on lung cancer cell line and tracking of Zn(II) ion in Zebra fish embryos	This Work

References

1. S. Goswami, D. Sena , N. K. Dasa , H-K Funb and C. K. Quah *Chem. Commun.*, 2011,**47**, 9101.
2. R. Joseph, B. Ramanujam, H. Pal and C. P. Rao *Tetrahedron Letters* 2008, **49**, 6257.
3. L. K. Kumawat and V. K. Gupta *Int. J. Electrochem. Sci.,* 2016, 11, 8861.
4. G. J. Park, J. J. Lee, G. R. You, L.T. Nguyen, I. Noh and C. Kim *Sens. Actuators. B,* 2016, **223,** 509
5. A. Jana, B. Das, A. R. Khuda-Bukhsh, S. K. Mandal, S. Mabhai and S. Dey *NewJ. Chem.,* 2016, **40**, 5976
6. S.Y. Lee, S. Y. Kim, J. A. Kim and C. Kim *J.Lumin* 2016, **179,** 602
7.U. Fegade, J. Marek, R. Patil, S. Attarde and A. Kuwar *J.Lumin* 2014, **146,** 234.
8. L. Qu, C. Yin, F. Huo, J. Chao, Y. Zhang and F. Cheng *Sens. Actuators. B,* 2014, **191,** 158.
9. R. Kavitha and T. Stalin *J. Lumin* 2015, **158,** 313
10. M. Shyamal, P. Mazumdar, S. Maity, S. Samanta, G. P. Sahoo and A. Misra *ACS Sens*. 2016, **1**, 739